A Mathematical Model of Wave Interaction with a Double Wall Barrier

P. Tillman[a], R. Cox[b] and B. Cathers[b]

[a] *School of Information Studies, Charles Sturt University, Wagga Wagga, NSW 2678, Australia (Present email: Pei.Tillman@csiro.au)*

[b] *Water Research Laboratory, School of Civil and Environmental Engineering, University of NSW, NSW 2093, Australia (r.cox@unsw.edu.au, b.cathers@unsw.edu.au)*

Abstract: Wave absorbing structures are widely used in harbour and offshore engineering. Breakwaters provide protection for harbours and floating marina facilities. The flow characteristics on the seaward and leeward sides of a structure are not only important for harbour protection, but also for the stability of the structure. Breakwater design can significantly influence wave reflection, wave transmission, wave induced forces and moments. The interaction between waves and the structure is a major concern of engineers in the design of breakwaters and wave barriers. In this paper, an eigenfunction expansion, numerical model is presented, which simulates wave interaction with a thin, vertical, double-walled, rigid wave barrier. The barrier partially penetrates the water column from the water surface down. The mathematical analysis is based on linear wave theory, supplemented by the appropriate external and internal boundary conditions to determine the velocity potential throughout the flow domain. The model predicts the influence of various wave barrier characteristics (such as wall penetration ratio and the spacing between two walls) on the performance of the barrier over a broad range of water depths and wave conditions. The results from the model include the reflection and transmission coefficients and relative amplitudes of the waves between the two barriers. The main advantage of this model is that it allows the analysis of the temporal kinematics and dynamics in the flow region. The present numerical solutions are compared with the experimental and numerical results from the literature.

Keywords: Water waves; Surface piercing wave barrier; Reflection; Transmission; Eigenfunction method

1. INTRODUCTION

Wave absorbing structures have been widely used along shorelines, channel entrances, beaches and marinas for long time. The primary function of wave barriers is to provide shelter by reducing the wave energy transmitted to the leeward side. The functional efficiency of these structures is evaluated by calculating the reflection and transmission of waves. The interaction between waves and the structure is a major concern of engineers in the design of breakwaters and wave barriers. Sometimes the appropriate design of wave barriers can virtually eliminate reflections and give rise to a substantial reduction of impact wave loads. As water depth increases, a wave barrier that further penetrates the water column becomes increasingly uneconomical, and a submerged breakwater may be used instead. In this study, a mathematical analysis is undertaken for predicting the performance of double, thin walled wave barriers that extend from above the water surface to some depth below, over a broad range of wave conditions.

Approximate analytical solutions of the transmission and reflection coefficients to this problem with infinite water depth can be found in Srokosz and Evans [1979] and Newman [1974]. These analytical solutions are based on irrotational, linear wave theory. Srokosz and Evans's [1979] wide-spacing approximation is based on the assumption that the barriers are spaced sufficiently far apart for the local wave field in the vicinity of one barrier not to influence the flow field near the other barrier. The only interaction between the barriers is due to the propagating-wave terms which occur in the scattering problem for a single barrier. Newman's solution [1974] is applied to cases with small separation between the plates and he assumed that the fluid motion between the plates is a uniform vertical oscillation. Stiassnie et al. [1986] conducted wave flume experiments to test the wide spacing approximation analysis. Wu and Liu

[1988] presented the method of matched eigenfunction functions at the barriers to find numerical solutions of the transmission and reflection coefficients for obliquely incident water waves with two floating rectangular cylinders.

In this study, the numerical model of eigenfunction expansion for double wall, thin wave barriers is developed to expand the applications of the analytical solutions mentioned above. The model not only provides transmission and reflection coefficients, but also the spatial and temporal flow field throughout the fluid domain. The theoretical formulation of the problem is described in the following section.

2. THEORETICAL FORMULATION

A regular, small amplitude, incident wave train of height H and angular frequency σ propagates in water of constant depth d past a double, thin vertical breakwater as shown in Figure 1. The origin of the coordinate system is taken at the still water level at the location of the first barrier with the x-axis horizontal and the z-axis vertical and pointing upwards. The fluid domain is divided into three regions: Region I for $x \le 0$, Region II for $0 \le x \le b$ and region III for $x \ge b$.

The fluid is assumed to be inviscid and incompressible, and the fluid motion is irrotational. Its velocity potential $\Phi(x,z,t)$ is:

$$\Phi(x,z,t) = \mathrm{Re}[\,\phi(x,z)e^{-i\sigma t}] \qquad (1)$$

where Re denotes the real part of the complex number, $i = \sqrt{-1}$, wave angular frequency $\sigma = 2\pi/T$, T = wave period. The fluid velocity vector is given by $V = \nabla \Phi$.

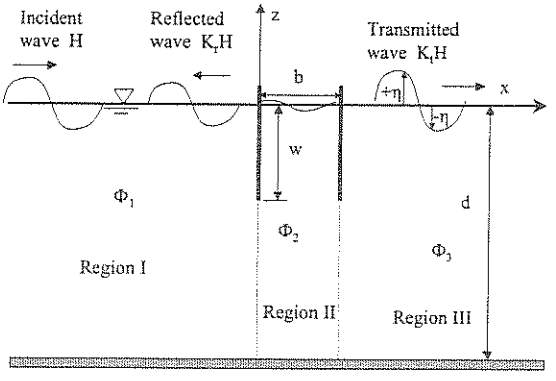

Figure 1. Definition sketch of a double wall wave barriers

The time-independent velocity potential $\phi(x,z)$ must satisfy the following equations:

Mass conservation in the flow region:

$$\frac{\partial^2\phi}{\partial^2 x} + \frac{\partial^2\phi}{\partial^2 z} = 0 \qquad (2)$$

No flow boundary condition on the seabed:

$$\frac{\partial\phi}{\partial z} = 0 \qquad \text{at } z = -d \qquad (3)$$

Free water surface boundary condition:
At the water surface, the pressure p = 0. From the Bernoulli equation,

$$\frac{\partial\Phi}{\partial t} + \frac{p}{\rho} + gz = 0 \qquad (4)$$

The water surface level ($z = \eta$) can be determined from

$$\eta = -\frac{1}{g}\frac{\partial\Phi}{\partial t}\Big|_{z=0} \qquad \text{at } z = 0 \qquad (5)$$

Taking the derivative with respect to t on both sides of Equation (5), we obtain

$$\frac{\partial\eta}{\partial t} = -\frac{1}{g}\frac{\partial^2\Phi}{\partial t^2}\Big|_{z=0} \qquad (6)$$

where $\frac{\partial\eta}{\partial t}$ represents the vertical fluid velocity v at the water surface, ie.

$$v = \frac{\partial\eta}{\partial t} = \frac{\partial\Phi}{\partial z}\Big|_{z=0}$$

From Equation (1),

$$\frac{\partial\Phi}{\partial t} = -i\sigma\Phi \qquad (7)$$

Substituting $\frac{\partial\eta}{\partial t} = \frac{\partial\Phi}{\partial z}$ and $\frac{\partial^2\Phi}{\partial t^2} = \sigma^2\Phi$ into Equation (6), we obtain

$$\frac{\partial\Phi}{\partial z} - \frac{\sigma^2}{g}\Phi = 0 \qquad \text{at } z = 0 \qquad (8)$$

Equation (8) is the free water surface boundary condition.

No flow boundary condition at the wave barriers:

$$\frac{\partial\phi}{\partial x} = 0 \qquad \text{at } x = 0 \text{ and } x = b,\ -w \le z \le 0 \qquad (9)$$

The energy associated with an incoming wave which encounters a wave barrier will be partially transmitted and reflected. The resulting wave motion in region I consists of an incident and a reflected wave while in region II, the wave motion is due to transmitted and reflected waves and in region III, the wave motion is due to transmitted wave only. The general solution for the velocity potential satisfying the above conditions

(Equations (2), (3) and (8)) in each region can be written as follows:

Region I ($x \le 0$):

$$\phi_1 = I_1 e^{ik_1 x} + \sum_{n=1}^{N} R_n I_n(z)\, e^{-ik_n x} \qquad (10)$$

Region II ($0 < x \le b$):

$$\phi_2 = \sum_{n=1}^{N} I_n(z)\,(A_n e^{ik_n x} + B_n e^{-ik_n (x-b)}) \qquad (11)$$

Region III ($x > b$):

$$\phi_3 = \sum_{n=1}^{N} T_n I_n(z)\, e^{ik_n (x-b)} \qquad (12)$$

where

$$I_n(z) = -\frac{igH}{2\sigma}\frac{\cosh[k_n(d+z)]}{\cosh(k_n d)} \qquad (13)$$

for n=1, 2, ...N

$k_1 = \frac{2\pi}{L}$ (wave number), L = wave length (m), H = incident wave height (m), d = water depth (m) R_n, A_n, B_n and T_n = complex coefficients describing the dimensionless amplitude and phase of the progressive (n=1) and evanescent wave modes (n>1), N-1= number of evanescent modes. The first term represents the incident wave, and the summation terms represent the scattered wave modes. The velocity potential of the actual incident progressive wave is described by:

$$\Phi_1 = I_1 e^{i(k_1 x - \sigma t)} \qquad (14)$$

The reflection and transmission coefficients for the progressive wave modes are given by:

$$K_r = |R_1|, \quad K_t = |T_1| \qquad (15)$$

The k_n in Equations (10) to (14) are determined from the following dispersion equation:

$$\sigma^2 = g k_n \tanh(k_n d) \qquad n = 1, 2, \ldots\ldots N \qquad (16)$$

where k_1 is the first real positive root, which is the wave number of a linear progressive wave number. k_n (n>1) are an infinite set of positive purely imaginary roots corresponding to evanescent waves travelling in both directions away from the barrier.

The velocity potentials ϕ_1, ϕ_2 and ϕ_3 must satisfy the internal boundary conditions at the wave barrier.

Internal Boundary Conditions

(1) No horizontal flow normal to the barrier,

$$\frac{\partial \phi_1}{\partial x} = \frac{\partial \phi_2}{\partial x} = 0, \quad \text{at } x = 0 \text{ and } -w < z < 0$$
$$\frac{\partial \phi_2}{\partial x} = \frac{\partial \phi_3}{\partial x} = 0, \quad \text{at } x = b \text{ and } -w < z < 0 \qquad (17)$$

(2) Applying pressure continuity below each barrier

$$\phi_1 = \phi_2 \quad \text{at } x = 0, -d < z < -w$$
$$\phi_2 = \phi_3 \quad \text{at } x = b \; -d < z < -w \qquad (18)$$

and velocity continuity

$$\frac{\partial \phi_1}{\partial x} = \frac{\partial \phi_2}{\partial x}, \quad \text{at } x = 0, -d < z < -w$$
$$\frac{\partial \phi_2}{\partial x} = \frac{\partial \phi_3}{\partial x}, \quad \text{at } x = b, -d < z < -w \qquad (19)$$

Now we are going to find four expressions to represent the boundary conditions in Equations (17) to (19). The mixed boundary condition can be defined as a function $G_1(z)$.

$$G_1(z) = \begin{cases} \phi_{1,x} = 0, & x = 0, -w \le z \le 0 \\ \phi_{2,x} - \phi_{1,x} = 0, & x = 0, -d \le z \le -w \end{cases} \qquad (20)$$

From the definitions of velocity potential ϕ_1, ϕ_2 and ϕ_3, the split function $G_1(z)$ can be described as

$$G_1(z) = \begin{cases} k_1 I_1(z) - \sum_{n=1}^{N} k_n R_n I_n(z) = 0, \\ \text{for } x = 0, -w < z < 0 \\ -k_1 I_1(z) + \sum_{n=1}^{N} k_n I_n(z)\left[R_n + A_n - B_n e^{ik_n b}\right] = 0, \\ \text{for } x = 0, -d < z < -w \end{cases} \qquad (21)$$

In the expression $G_1(z) = 0$, the complex coefficients R_n, A_n and B_n are unknown and need to be determined. Once all these values are solved, the solution of the velocity potential is found. $G_1(z)$ satisfies a certain integral equation. $G_1(z) = 0$ can be satisfied along the whole water column by employing the orthogonality properties of the depth-dependent eigenfunctions $I_n(z)$. This means integrating the product of $G_1(z)$ and the depth-dependent eigenfunctions $I_n(z)$ with respect to z and setting the result to zero. Elimination of z from the resulting integral equation then makes the solution for R_n, A_n and B_n possible. Therefore,

$$\int_{-d}^{0} G_1(z) I_m(z) dz = \int_{-d}^{-w} G_1(z) I_m(z) dz + \int_{-w}^{0} G_1(z) I_m(z) dz$$
$$= \int_{-d}^{-w} (\phi_{2x} - \phi_{1x}) I_m(z) dz + \int_{-w}^{0} \phi_{1x} I_m(z) dz = 0 \qquad (22)$$

Equation (22) can be recast in matrix form as a set of linear equations:

$$\sum_{n=1}^{N} E_{nm} R_n + \sum_{n=1}^{N} C_{nm} A_n + \sum_{n=1}^{N} D_{nm} B_n = F_m, \qquad m = 1, 2, \ldots N \tag{23}$$

where $C_{nm} = k_n f_{nm}(-d,-w)$,

$D_{nm} = -k_n e^{ik_n b} f_{nm}(-d,-w)$,

$E_{nm} = k_n f_{nm}(-d,-w) - k_n f_{nm}(-w,0)$,

$F_m = k_1 f_{1m}(-d,w) - k_1 f_{1m}(-w,0)$,

$f_{nm}(\alpha,\beta) = \int_{\alpha}^{\beta} I_n(z) I_m(z) dz$

From pressure continuity at x=0, -d≤z≤-w, $\phi_1 = \phi_2$, we can obtain the second boundary condition function $G_2(z)$.

$$G_2(z) = \begin{cases} \phi_{2,x} = 0 & x = 0, -w \le z \le 0 \\ k_1(\phi_2 - \phi_1) = 0 & x = 0, \ -d \le z \le -w \end{cases}$$

or

$$G_2(z) = \begin{cases} \sum_{n=1}^{N} ik_n I_n(z)\left[A_n - B_n e^{ik_n b}\right] = 0, \\ \text{for } x = 0, -w \le z \le 0 \\ -k_1 I_1(z) + k_1 \sum_{n=1}^{N} I_n(z)[-R_n + A_n + B_n e^{ik_n b}] = 0, \\ \text{for } x = 0, -d \le z \le -w \end{cases} \tag{24}$$

Following a similar procedure applied to $G_1(z)$ previously, we employ the orthogonality properties of the depth-dependent eigenfunctions $I_n(z)$ to eliminate z from $G_2(z)$. Therefore,

$$\int_{-d}^{0} G_2(z) I_m(z) dz = \int_{-d}^{-w} G_2(z) I_m(z) dz + \int_{-w}^{0} G_2(z) I_m(z) dz = 0$$

We obtain the second matrix form of linear equations containing R_n, A_n and B_n as

$$\sum_{n=1}^{N} L_{nm} R_n + \sum_{n=1}^{N} G_{nm} A_n + \sum_{n=1}^{N} H_{nm} B_n = O_m, \qquad m = 1, 2, \ldots N \tag{25}$$

where $G_{nm} = k_1 f_{nm}(-d,-w) + ik_n f_{nm}(-w,0)$,

$H_{nm} = k_1 e^{ik_n b} f_{nm}(-d,-w) - ik_n e^{ik_n b} f_{nm}(-w,0)$,

$L_{nm} = -k_1 f_{nm}(-d,-w)$, $O_m = k_1 f_{1m}(-d,-w)$

From the mixed internal boundary conditions at the second barrier, x = b, we can form the third and fourth boundary condition functions:

$$G_3(z) = \begin{cases} \phi_{2,x} = 0, & x = b, -w \le z \le 0 \\ \phi_{3,x} - \phi_{2,x} = 0, & x = b, -d \le z \le -w \end{cases} \tag{26}$$

$$G_4(z) = \begin{cases} \phi_{3,x} = 0 & x = b, -w \le z \le 0 \\ k_1(\phi_3 - \phi_2) = 0 & x = b, -d \le z \le -w \end{cases} \tag{27}$$

From Equations (26) and (27), we obtain the following matrix form of linear equations containing unknown coefficients R_n, A_n, B_n and T_n.

$$\sum_{n=1}^{N} P_{nm} A_n + \sum_{n=1}^{N} Q_{nm} B_n + \sum_{n=1}^{N} S_{nm} T_n = 0 \tag{28}$$

$$\sum_{n=1}^{N} U_{nm} A_n + \sum_{n=1}^{N} V_{nm} B_n + \sum_{n=1}^{N} W_{nm} T_n = 0 \tag{29}$$

where

$P_{nm} = k_n e^{ik_n b}\left[f_{nm}(-w,0) - f_{nm}(-d,-w)\right]$,

$Q_{nm} = -k_n f_{nm}(-w,0) + k_n f_{nm}(-d,-w)$,

$S_{nm} = k_n f_{nm}(-d,-w)$, $U_m = -k_1 e^{ik_n b} f_{nm}(-d,-w)$,

$V_{nm} = -k_1 f_{nm}(-d,-w)$,

$W_{nm} = ik_n f_{nm}(-w,0) + k_1 f_{nm}(-d,-w)$

Solving the system of linear complex equations (23), (25), (28) and (29) yields the complex amplitudes R_n, A_n, B_n and T_n (n = 1, …N). The reflection and transmission coefficients are given by Equation (15).

3. SIMULATION RESULTS AND ANALYSIS

Eq.(23), (25), (28) and (29) constitute 4N simultaneous equations for the unknown complex coefficients R_n, A_n, B_n and T_n (n = 1, 2, …N). These equations were solved using the mathematical software MAPLE V by Waterloo Inc. [Ellis et al., 1997]. We conducted numerical experiments for (i) closely spaced barriers with b = 0.2w; (ii) widely spaced barriers, where the spacing ratio is b = 3w.

Close barrier spacing cases (b/L= 0.01~0.05)

The limiting case of close spacing for two barriers is one wave barrier. In order to guarantee the accuracy of the present method, the numerical tests for the close spacing case such as b=0.2w was carried out and the results were compared with the analytical and numerical solutions from the literature for a single barrier. The test conditions were water depth d = 20m, barrier penetration ratio w/d = 0.1, distance between two barriers b = 0.2w and wave period T = 2.2 ~ 5.2s. The relative barrier spacing b/L varies from 0.01 ~ 0.05 and

d/L = 0.48 ~ 2.55. The present predicted transmission and reflection coefficients with 1 and 10 modes are shown in Figures 2 and 3. Also shown for comparison are the corresponding values of K_t and K_r from the modified power transmission theory (MPTT) [Kriebel and Bollmann, 1996] and the eigenfunction solution (N=20) for the single barrier [Tillman et al., 2001]. These figures give credence to the accuracy of the present method. For long wavelengths or small barrier spacings the transmission coefficient is increased relative to the single barrier values, whereas for short wavelengths or large barrier spacing the transmission coefficient is reduced by the presence of the second barrier.

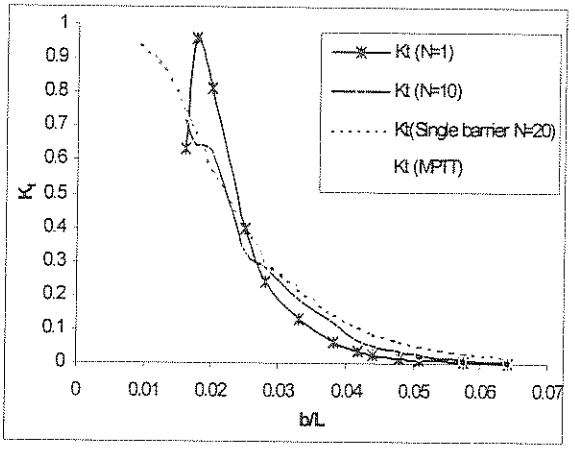

Figure 2. Transmission coefficient for incident waves impinging on a double wall barrier with w/d =0.1, b/w = 0.2.

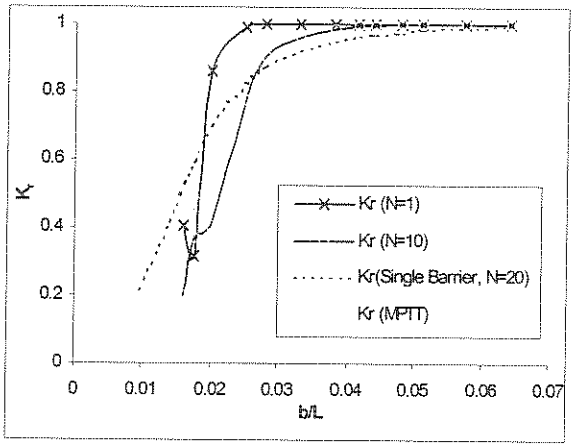

Figure 3. Reflection coefficient for incident waves impinging on a double wall barrier with w/d =0.1, b/w= 0.2.

Wide barrier spacing cases (b/L= 0.13~0.70)

Numerical results were obtained for the same geometry as in an experiment by Stiassnie et al. [1986] with d=0.775m, w=0.2m, penetration ratio w/d = 0.258. By changing the wave period T from 0.74 to 2.0 seconds, the ratio b/L is in the range of 0.13~ 0.7 and relative water depth d/L varies from 0.3 (intermediate water) to 1.3 (deep water). The comparison between current numerical results for the predicted transmission and reflection coefficients with the number of modes N=1, 5 and 10 and Stiassnie's experimental data [Stiassnie et al., 1986] is shown in Figures 4 and 5. It indicates that the eigenfunction solution approaches the experimental results with increasing number of modes. There is reasonable agreement between the numerical results with N=10 and the experimental data. The results show that for long wavelengths or small barriers spacings the transmission coefficient is higher, whereas for short wavelengths or large barriers spacings the transmission coefficient is lower.

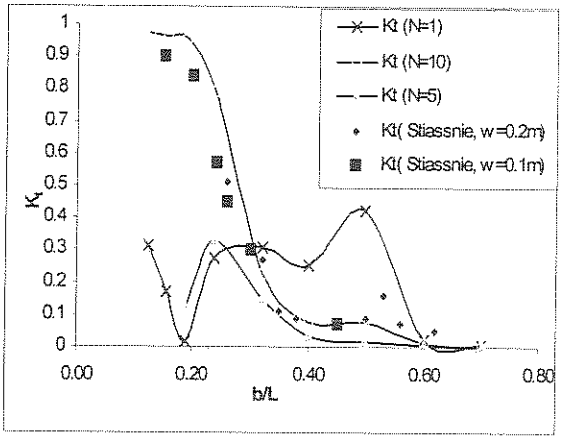

Figure 4. Transmission coefficient for incident waves impinging on a double wall barrier with w/d=0.258, b/w=3.

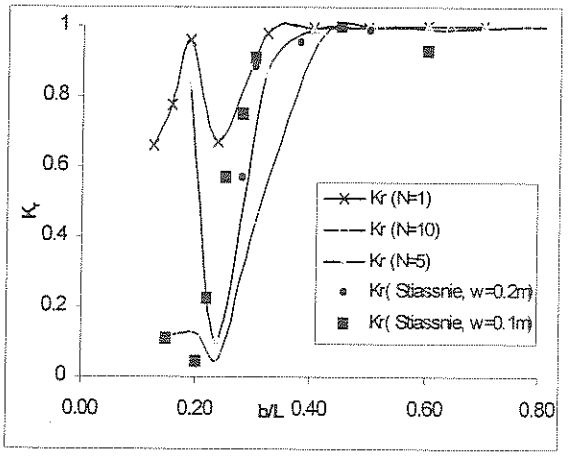

Figure 5. Reflection coefficient for incident waves impinging on a double wall barrier with w/d=0.258, b/w=3.

The present numerical model is able to provide the overall flow profile for the fluid domain (see Figure 6). The free water surface elevation versus time on both sides of the wave barriers is plotted in

Figure 7. The graph shows wave amplitudes as well as phase shifts on both sides of the wave barriers. This information is of particular importance in engineering design for the calculation of the forces and moments on the wave barriers.

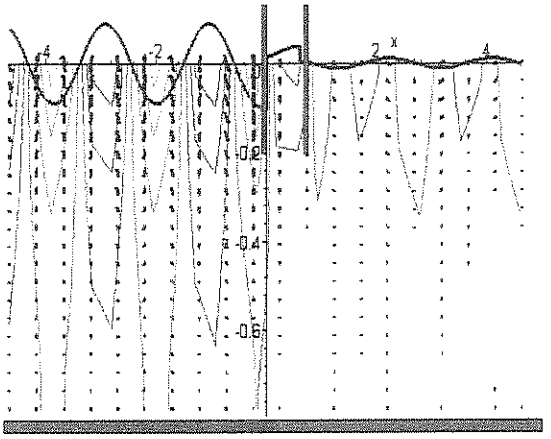

Figure 6. Water surface profile, velocity potential and flow field for the case: d = 0.775m, w = 0.2m, w/d = 0.258, b = 3w, T = 1.1s, d/L = 0.415, b/L = 0.321.

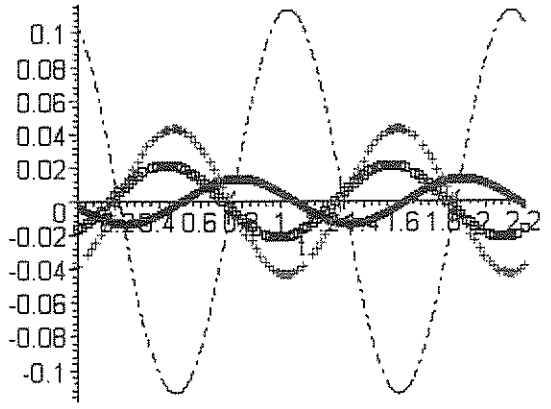

Figure 7. Free water surface against time on both sides of the wave barriers for the same case illustrated in Figure 6:
d = 0.775m, w = 0.2m, w/d = 0.258, b = 3w, T = 1.1s, d/L = 0.415, b/L = 0.321.
- - - η_1 at x=0, at the front of the barrier No.1;
+++ η_2(x=0), at the back of the barrier No.1;
□□□ η_2(x=b), at the front of the barrier No.2;
— η_3(x=b), at the back of the barrier No.2.

4. CONCLUSIONS

The method of eigenfunction expansion is developed to examine the performance of two thin vertical wave barriers. The numerical results reported in this paper indicate that the present eigenfunction expansion method works well for the thin, double wall wave barrier configuration provided about ten wave modes are included in the analysis. The experimental data and numerical/analytical solutions from the literature generally agree with this numerical model approach. While the transmission coefficient decreases for long wavelengths or large barrier spacing, the reflection coefficient increases. For short wavelengths or large spacing between barriers, the breakwater system with two vertical barriers shows an improvement over the system with one vertical barrier. The present model demonstrates its capacity to reproduce and enable animation of the water motion in and around the double wall wave barrier. It provides important information for the calculation of forces and moments on the wave barriers in engineering design.

5. ACKNOWLEDGMENT

This study has been supported by the Special Study Program, Charles Sturt University.

6. REFERENCES

Ellis, W., Jr. E. Johnson, E. Lodi and D. Schwalbe, *Maple V Flight Manual Release 4, Tutorials for calculus, linear algebra, and differential equations*, Brooks/Cole Publishing Company, 168pp, 1997.

Kriebel, D. L. and C. A. Bollmann, Wave transmission past vertical wave barriers, *International Conference on Coastal Engineering ASCE*, Orlando, 2470-2471, September, 1996.

Newman, J. N., Interaction of water waves with two closely spaced vertical obstacles, *J. Fluid Mech.*, 66, 97-106, 1974.

Srokosz, M. A. and D. V. Evans, A theory for wave-power absorption by two independently oscillating bodies, *J. Fluid Mech.*, 90, 337, 1979.

Stiassnie, M., I. Boguslavsky, and E. Naheer, Scattering and dissipation of surface waves by a bi-plate structure, *Applied Ocean Research*, Vol.8, No.1, 33-37, 1986.

Tillman, P., R. Cox, and B. Cathers, The performance of a thin impermeable waver barrier assessed by the eigenfunction method, Submitted to *Journal of Engineering Mathematics*, 2001.

Wu, J., and P. Liu, Interactions of obliquely incident waves with two vertical obstacles, *Applied Ocean Research*, 10(2), 66-72, 1988.